TECHNICAL PUBLICATION

Thermal aspects of flange-mounted r.f. power transistors

TECHNICAL NOTE 141

Philips
Semiconductors

PHILIPS

CONTENTS

1 INTRODUCTION

R.F. power transistors often operate under conditions of severe mismatch. This often increases collector dissipation and consequently junction temperature. Failure mechanisms in high power transistors (breakdown, degradation, electromigration, thermal fatigue) are highly temperature dependent, so proper attention must be paid to their thermal conditions. However, it is an area where calculations are difficult and misunderstandings abound; this article is intended to clear up some of the misunderstandings and correct a number of misconceptions.

2 PRACTICAL POINTS:

- The central area of the flange directly under the crystal contributes much less to heat transfer than has hitherto been thought; it is the area under and around the mounting bolt heads that conducts the bulk of the heat away.
- Although lapping the contacting surfaces of both heatsink and flange does improve thermal conductivity, the improvement is less than if a very thin layer of heatsink compound is used.
- Both of the commonly used bolts (M3 and UNC4-40) provide sufficient pressure when torqued to between 0,6 and 0,75 Nm. Using higher torques with a view to improving thermal contact resistance is counterproductive. Thermal contact resistance is more likely to increase.
- Except in the case of the UNC4-40 bolt, the maximum pressures encountered under these conditions do not cause excessive plastic deformation of the underside of the flange, and the minimum is sufficient to provide good thermal contact throughout life.

3 THERMAL MODELS

Many thermal models have been proposed in efforts to provide an analytical base from which to calculate the thermal behaviour of operating transistors. Because of the number of assumptions that have to be made, none survive comparison with actual measurements. Particularly with regard to hot-spotting and thermal contact resistance, theory and practice often differ by a factor of three.

The most dangerous assumption is probably that the chip surface temperature can be averaged and, therefore, that a uniform heat flux exists on the surface of the silicon chip. Although a large number of small base areas are distributed over the chip surface in order to promote even heat distribution, this assumption assigns too low a temperature to certain critical points on the chip surface. Because the hottest point presents the highest reliability risk, averaging leads to this risk being underestimated.

The situation is made clearer if we consider the power dissipation per unit area and the temperature gradients in and near the crystal of a high power transmitting transistor. In the crystal itself, in the base area a few micrometres under the emitter fingers the dissipation is about 500 W/mm^2 with a temperature gradient of about 5000 K/mm; in the BeO disc, about 5 W/mm^2 with a gradient of 25 K/mm; and in the flange, 2 W/mm^2 with a gradient of 5 K/mm. Efficient heat distribution is, therefore, essential if junction temperature is to be held below 200 °C.

Other assumptions that undermine the validity of current thermal models are: that heat distribution is uniform; and that the base of the transistor flange and the heatsink surface are isothermic.

Figures 1 to 6 show known models. These illustrate the difficulties of calculating thermal resistance when boundary conditions have to be assumed. It is clear that the influence of the finite thermal resistance of the heatsink is great, as is that of the mounting base. The most important result is that for a thick heatsink the contact area formed by the annulus between 0,8r and r largely determines the thermal resistance of the whole contact area. These results are confirmed by measurements (described in the “Appendix”) that show that removing metal from the flange centre barely affects the thermal resistance of the contact area. Other reasons for the bolt head are being important are discussed below.

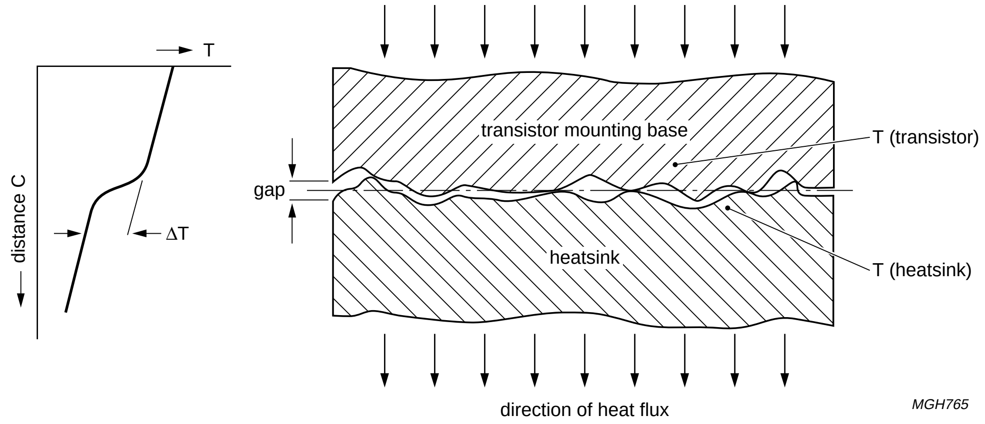

Fig.1 This rather simplified case is often mentioned in the literature to describe contact surface thermal resistance. It assumes a constant heat flux normal to the contact area. Thermal resistances can be calculated using the average gap between the surfaces (caused by micro-asperities, see Thermal contact) which is filled with air or heatsink compound. Ref. 1, 2.

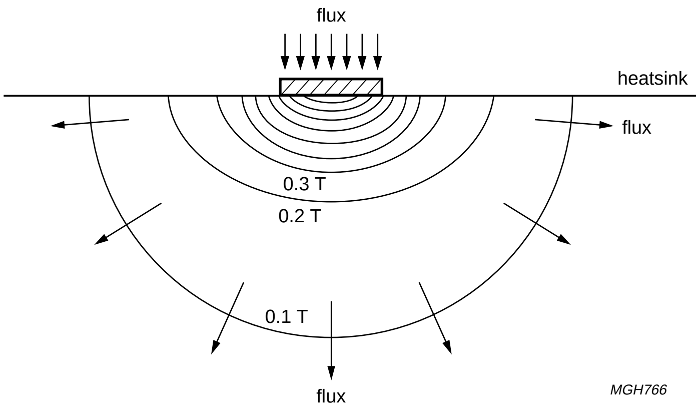

Fig.2 This theoretical approach assumes an infinite heatsink with a uniform constant heat flux normal to a circular contact area. The temperature distribution on the heatsink surface requires the solution of complete elliptic integrals. The results are plotted in Fig.3. The most important facts emerging from this approach are: the average angle of the heat flux in the heatsink is >60° to the direction of the assumed transistor heat flux; and that the thermal resistance of the heatsink is inversely proportional to the radius of the heat flux and not to the surface area of the heat flux. Ref. 3, 4.

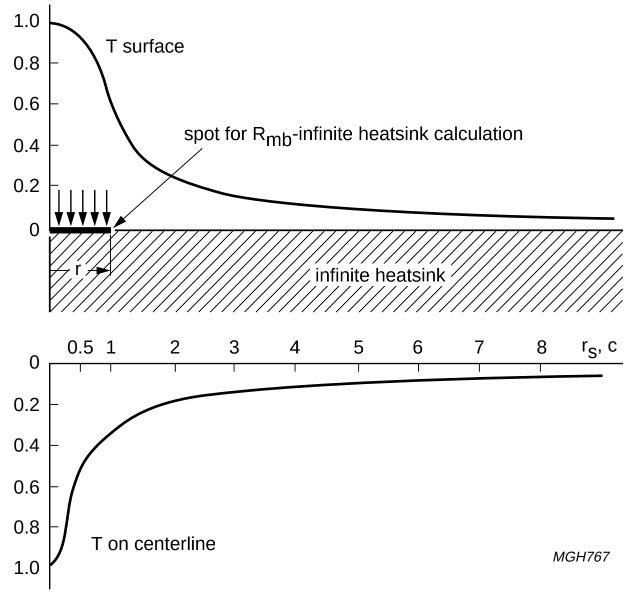

Fig.3 Temperature of (a) the heatsink surface and (b) the centre of the body of the heatsink normal to the surface, as calculated using the approach of Fig.2.

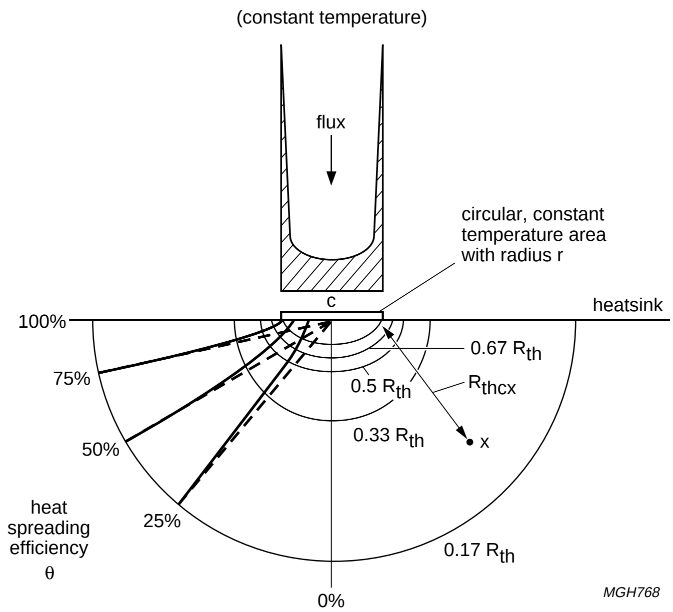

Fig.4 This approach assumes a constant mounting base temperature and a low contact thermal resistance. This also requires the solution of complete elliptic integrals, but with a simpler result for calculating the temperature at a distance x from the centre; Ref. 5, 6. For large distances the results are the same as for Fig.2. For an elliptic contact area (or, with slight error, for a rectangular flange) a form factor can be applied. The main difference with Fig.2 is in the flux, which has infinite intensity at the edge of the contact area. The most important result of this is that 50% of the total heat flux passes through an annulus of r – 0,9r; i.e., if a circle of 0,9r is removed from the contact area, thermal resistance is only doubled.

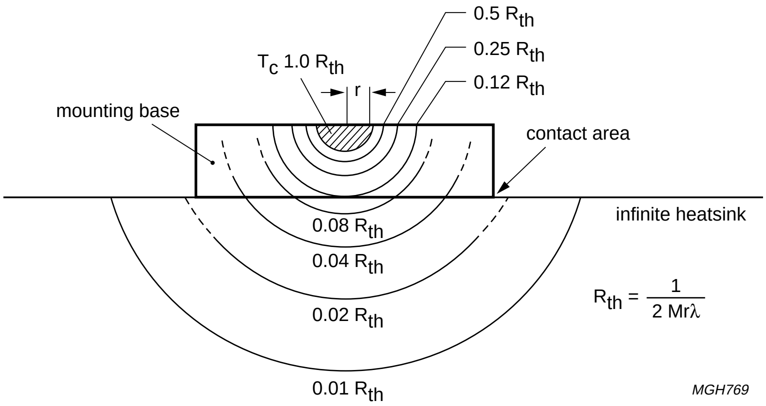

Fig.5 The fourth approach is to assume a small hemispherical heat source of constant temperature half buried in the upper surface of the flange. If flange and heatsink are of the same material and the thermal contact resistance is low, the isothermals will be hemispheres passing through flange and heatsink and temperature will decrease with the square of the distance.

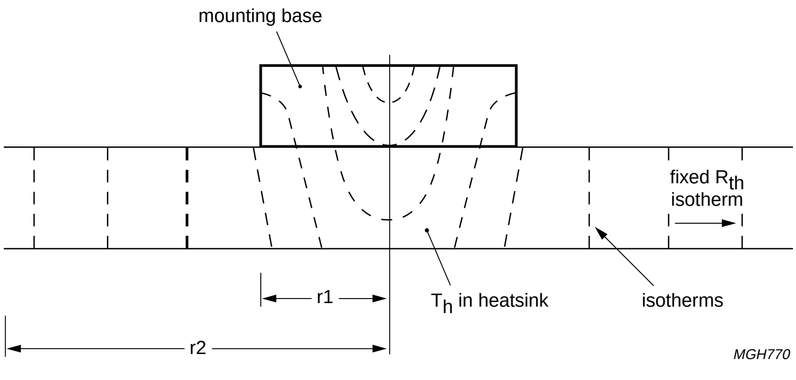

Fig.6 If, in the case of Fig.5 we assume the heatsink to be thin (thickness <r), the thermal resistance will be infinite if the heatsink is not connected to a point of fixed thermal resistance such as fins or water jacket. If, at a distance r2, such a (circular) connection does exist, the isotherms will be concentric circles on the surface of the heatsink and, if r2 ≈ 2r1, heat flux will decrease linearly with distance. The R_{th} of the transistor will be higher because the heat spreads differently.

4 SURFACE CONDITIONS

Because of irregularities in their surfaces two apparently flat objects will probably contact over less than a thousandth of their common surface area when pressed together. Three types of surface irregularity are of interest to us here:

- Waviness, i.e., deviation from flatness (see Fig.7(a)). This includes the plastic deformation of the transistor flange cause by the differing coefficients of expansion of BeO and Cu. After the BeO disc has been attached the two materials contract at different rates, setting up stresses that deform the flange, making it slightly concave. Although the flange is subsequently ground, residual stresses cause the copper to creep and the flange is therefore very slightly concave (typically 7 μm) when delivered (see Fig.15).
- Grooving, a repetitive form of deformation that is usually the result of milling, turning, grinding, etc. This is rarely a problem in transmitting transistor flanges but may occur in heatsink, especially those of poor quality. (See Fig.7(b)).
- Non-repetitive micro-asperities, a random phenomenon that is reduced but not entirely removed by lapping or polishing. It is characteristic of all normal surfaces. (Fig.7(c)).

Surface irregularities of the last two types are usually expressed in terms of average roughness (r_a), as shown in Fig.7(c). Instead of arithmetic average. The r.m.s. value (a slightly higher value) is often used in the USA. Although most suited to defining the smoothness of sliding surfaces, r_a does not indicate the intimacy of contact between two surfaces, which is what concerns us here. A more useful way of expressing roughness for our purposes, one rarely used for transistor flanges, would be that of DIN4762, i.e., the percent bearing surface (t_p) at a given depth (c). Figure 8 compares r_a and t_p for a selection of surface profiles.

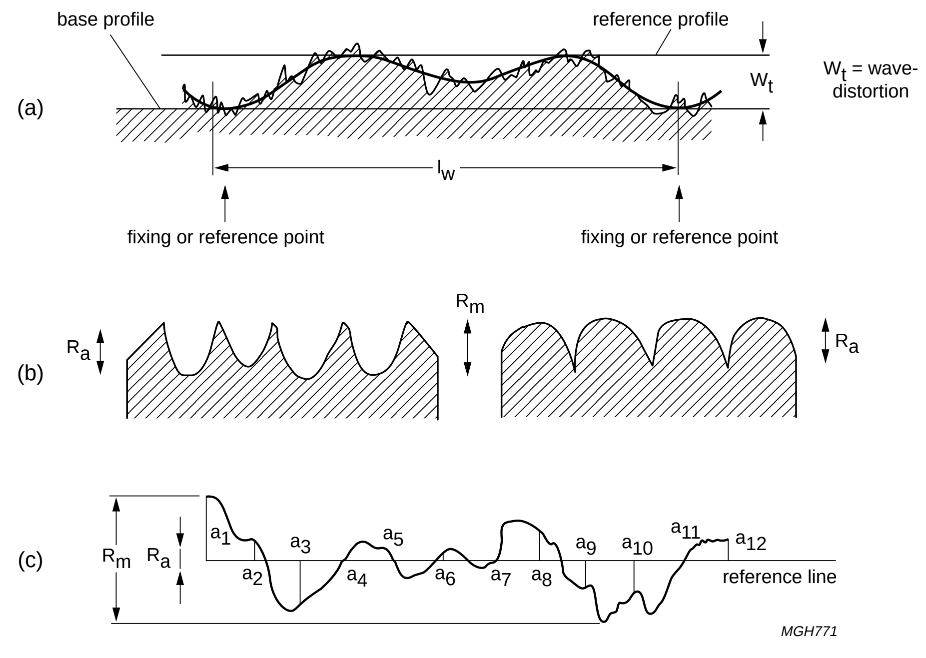

Fig.7 Three types of surface distortion of interest in thermal contacts. That of (a) can be cured by lapping or polishing whereas those of (b) and (c) can only be reduced.

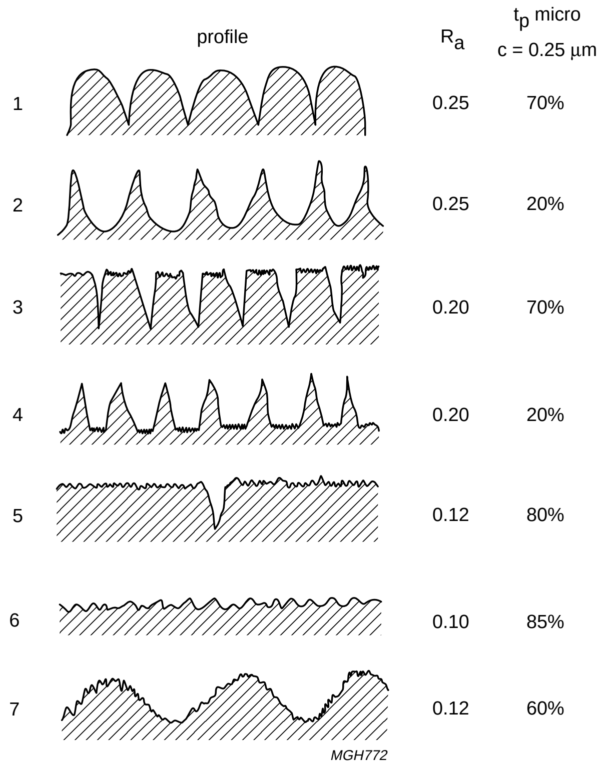

Fig.8 Although R_a is a good indication of the frictional behaviour of mating surfaces, it is less effective in defining the intimacy of contact as is needed for our purposes. A better indication is given by percent bearing surface, t_p, at a given depth, c, in this case 0,25 µm.

5 THERMAL CONTACT

From the foregoing it will be seen the contact conductance between two surfaces is the sum of the conductances of a very large number of metallic contacts in parallel with a similar number of air gaps (perhaps filled with heatsink compound). $R_{th\ mb\text{-}hs} = 1/h_t$ where $h_t = h_m + h_f$: h_m and h_f being the conductance of the metallic paths and of the air (or heatsink compound) paths, respectively.

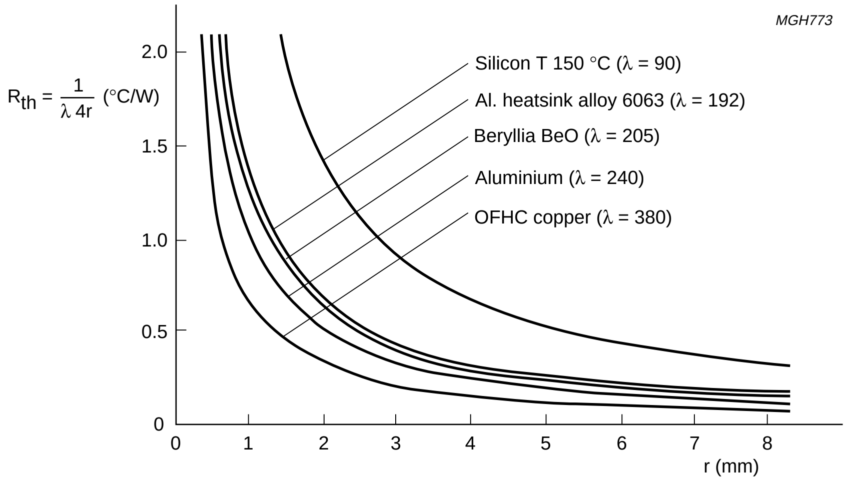

Fig.9 Thermal resistance of various materials as a function of distance measured from the edge of a circular heat flux into an infinite heatsink. The thermal resistance in the centre of the heath flux is higher by a factor of 1,57.

Of course, the contacting surfaces of heatsink and transistor flange will not remain unaffected by the pressure when the two are clamped together. Where the pressure is greatest the asperities will, naturally, be to some extent crushed, thus increasing the area of metallic contact at these point. It is worth examining how the applied pressure is distributed.

6 PRESSURE DISTRIBUTION

Because the transistor flange is flexible the pressure imparted by the clamping bolts is not distributed uniformly over it. Accurate calculation of the actual pressure distribution is impeded by a number of difficulties:

- The flange is not perfectly flat
- Its shape is irregular
- The modulus of elasticity is higher in the centre of the flange than elsewhere.

In fact about 90% of the clamping force is exerted in an area twice that of the screw head (or washer, if used). Away from this area the force falls rapidly, its approximate value being given by:

$$F = F_i\left(\frac{Ph^3}{L^3} + \frac{K}{L^3}\right)$$

here:

F = pressure

P = the product of modulus of elastically, mass moment of inertia, shape factor and roughness factor

K = waviness factor (which may be negative)

h = height of flange

L = distance from fixing point

F_i = force under bolt head.

Because the denominator includes the third power of the distance, pressure falls off rapidly with distance from the fixing point and may even become negative. This is confirmed by the fact that the centre of a transistor flange lifts away from the heatsink when too high a torque is applied to the bolts. Figure 10 illustrates how pressure is distributed over the flange. In the following we shall see what actual forces are involved.

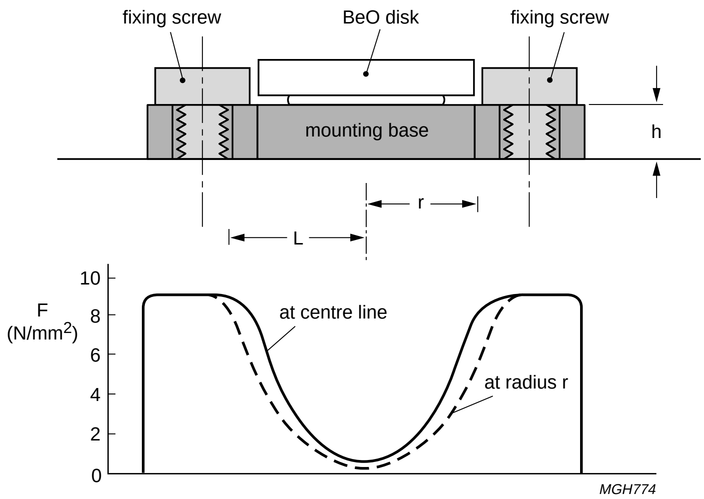

Fig.10 Pressure distribution over the mounting surface of an ideal (flat) flange. The highest pressure occurs round the bolt heads.

7 FORCE UNDER THE BOLT HEAD

The equation for clamping force would be simple were it not for the effect of friction. Friction enters in two ways: friction between bolt head and flange and friction between the external and internal screw threads. The coefficient of friction depends on the two materials in contact and the degree of lubrication. Table 1 shows the coefficient of friction for the materials of interest, the bolts being usually of steel and the heatsink either of copper or aluminium. Sometimes a steel nut is used.

Table 1

MATERIAL	COEFFICIENT OF FRICTION			
	UNLUBRICATED		LUBRICATED	
	MIN.	MAX.	MIN.	MAX.
steel – copper	0,5	0,8	0,2	0,6
steel – aluminium	0,5	1,3	0,2	0,6
steel – steel	0,3	0,7	0,1	0,2

Note: at higher contact pressures the coefficient of friction increases due to atomic adhesion and gouging.

The relation between torque and the force under the bolt head is:

$$F_i = \frac{2T}{D_m f_b + D_p \dfrac{\tan(B + \varnothing)}{\cos\alpha}}$$

where:

T = applied torque (0,6 to 0,75 newton metres)

D_m = mean bearing diameter of bolt (M3 = 4,2 mm; UNC4-40 = 3,9 mm)

D_p = pitch diameter of thread (M3 = 2,675 mm: UNC4-40 = 2,433 mm)

B = helix angle of thread (M3 = 3,41°; UNC4-40 = 4,77°)

f_b = coefficient of friction between bolt head and flange (0,5 – 0,8)

$\varnothing$ = friction angle ($\varnothing = \tan^{-1} f_t$, where f_t, the coefficient of friction between the screw threads, is 0,3 to 1,3)

α = half thread profile (30° for both threads).

Table 2 shows the maximum and minimum figures for the two bolts in question and the three materials into which the bolts are screwed. In all cases friction between bolt head and flange is assumed to be steel-to-copper. The minimum values were calculated using minimum torque and maximum coefficient of friction. Estimating probable maximum values is less straightforward. Friction will increase, even from the minimum value, as pressure increases. The chance of some lubricant (in the form of heatsink compound) being present is quite high, even if care is taken. On the basis of experience, we have taken a median value for coefficient of friction to arrive at the maximum force values in Table 2.

Table 2

MATERIAL INTO WHICH BOLT IS SCREWED	FORCE UNDER BOLT HEAD (NEWTONS)			
	M3		UNC4-40	
	MIN.	MAX.	MIN.	MAX.
copper	308	385	322	403
aluminium	308	385	322	403
steel	369	461	394	493

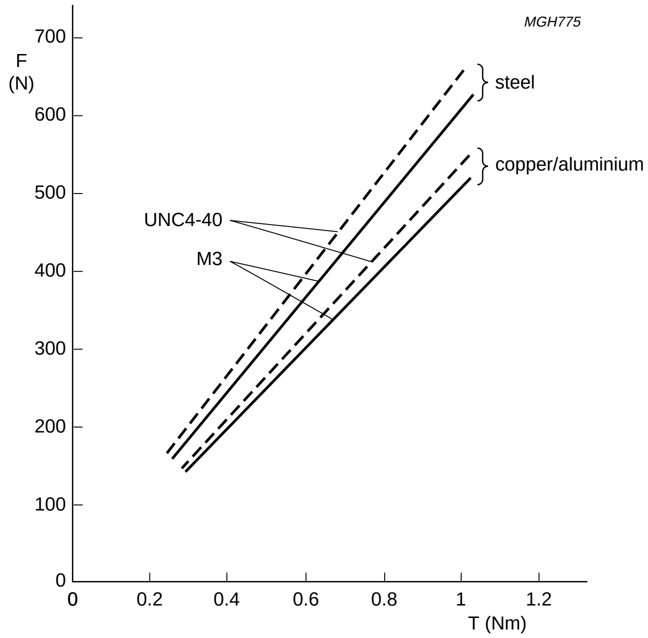

Fig.11 Force under the bolt head as a function of applied torque. Note that the UNC4-40 bolt gives a slightly higher force than the M3.

These results are plotted in Fig.11. The curves are extended to higher torque values to take account of torquing error. Depending on the type of tool used and the speed of operation, the bolts may be over-torqued by a factor of up to 1,6.

It is clear that the UNC4-40 bolt gives a somewhat higher force under the head than the M3. The difference in pressure is even greater because the UNC4-40 bolt head is smaller than the M3.

It should be borne in mind that the relation and curves are only valid up to certain limits. At some point the bolt head starts biting into the material under it and the threads start biting into each other. At the limit either the threads strip or the bolt shears. So, instead of being straight lines the curves will flatten out.

8 MOUNTING PRESSURE

We can derive the actual mounting pressure from the contact area between bolt head and flange.

Bearing area = bolt head area - flange hole area.

Minimum bearing area = minimum head area - maximum hole area.

Maximum bearing area = maximum head area - minimum hole area.

The lowest and highest pressures are then obtained by combining the above results with the force values from Table 2.

$$\text{Minimum pressure} = \frac{\text{minimum force}}{\text{maximum area}}$$

$$\text{Maximum pressure} = \frac{\text{maximum force}}{\text{minimum area}}$$

9 DEFORMATION

Metals, particularly copper which is highly ductile, deform when loaded. Up to a specific stress this deformation is elastic, i.e., remove the load and the metal returns to its original shape. Above this point permanent deformation occurs. Compared with metals such as steel, the elastic limit of copper is quite low; depending on its production history, plastic deformation can begin at stresses of about 20 N/mm^2.

The production history of the flange copper is not published. However it is reasonable to assume that it is cold rolled with some consequent work hardening. Brazing on the BeO disc at a temperature of about 800 °C will cause annealing. Under the disc, however, the differing expansion coefficients of copper and beryllium (18 compared with 5,8) will cause stresses. The copper, being the more ductile of the two, will deform with consequent work hardening around the centre. Machining flat will also cause some work hardening. The result is that the material properties of the flange lie somewhere between those of cold drawn copper and fully annealed copper.

Figure 12 shows the probable stress/strain curve for these conditions. Inserting the stress values obtained in Table 3, we get the expected degree of deformation. The highest stresses occurring with M3 bolts (±35 N/mm^2) are just over the border of elastic deformation (strain not exceeding 0,05%). Even with a factor of 1,6 to allow for over-torquing we are still within safe limits, below, say, 0,08%. With UNC4-40 the stresses are much higher than this and, if an allowance of 1,6 is made for torquing error, strains of up to 1,0% (and not less than 0,04%) are likely. Where possible this should be avoided, if necessary by fitting a 5,5 mm washer under the head.

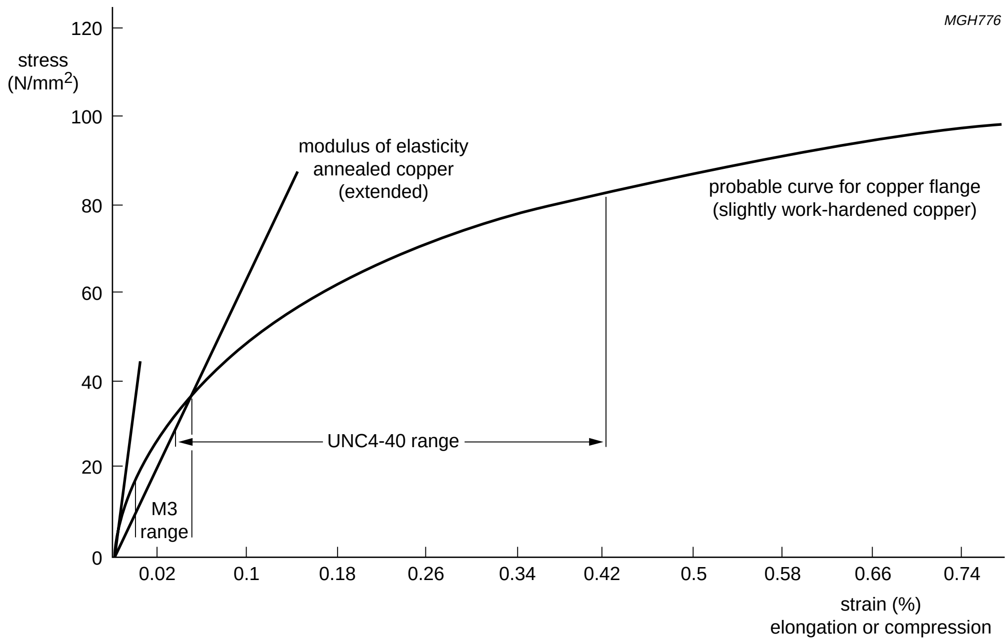

Fig.12 Stress/strain curve for the copper flange. The smaller head diameter of the UNC4-40 bolt leads to much higher strains than with the M3. When maximum torque is applied a washer will reduce strain to an acceptable level.

Table 3 Pressure in newtons/mm^2; note 1

MATERIAL	M3		UNC4-40	
	MIN.	MAX.	MIN.	MAX.
copper	18	29	30	68
aluminium	18	28	30	68
steel	22	35	36	83

Note

1. 1 newton/mm^2 = 1 MPa.

10 EFFECTS OF DEFORMATION

Because the copper flange is compressed between bolt head and heatsink, displaced metal can only escape radially. Some will escape toward the centre, but most will flow outward. Along the axis between the bolts two stresses will be operating from opposite directions. The metal can only escape by lifting the centre of the transistor flange away from the heatsink, as shown in Fig.13.

Figure 14 shows the result of tests in which a flange was mounted by high tensile steel M3 bolts to a thick tool-steel heatsink with polished surface. The M3 bolts were screwed into steel nuts, a friction coefficient of about 0,3 being applicable. The torque on the bolts was increased in steps of 0,2 Nm from an initial 0,4 Nm. After each step the flatness was measured along the dotted line. The enlarged curve for a torque of 0,8 Nm shows that the centre of the flange has lifted by 7 μm. This lifting will increase contact thermal resistance and as, in any case, normal heatsink are not perfectly flat, it is clear that torques of 0,75 Nm should not be exceeded. It is worth nothing that even though the tests extended to torques as high as 2,0 Nm, in no case was a beryllium oxide disc damaged.

Among the conclusions to be drawn from the above are that high torques do not improve contact thermal conductivity and that once a transistor has been mounted it should never be removed to another heatsink. For one thing it has adapted to the footprint of the heatsink it was first mounted on, and further, because of tolerances, the pitch of the mounting hole threads will differ.

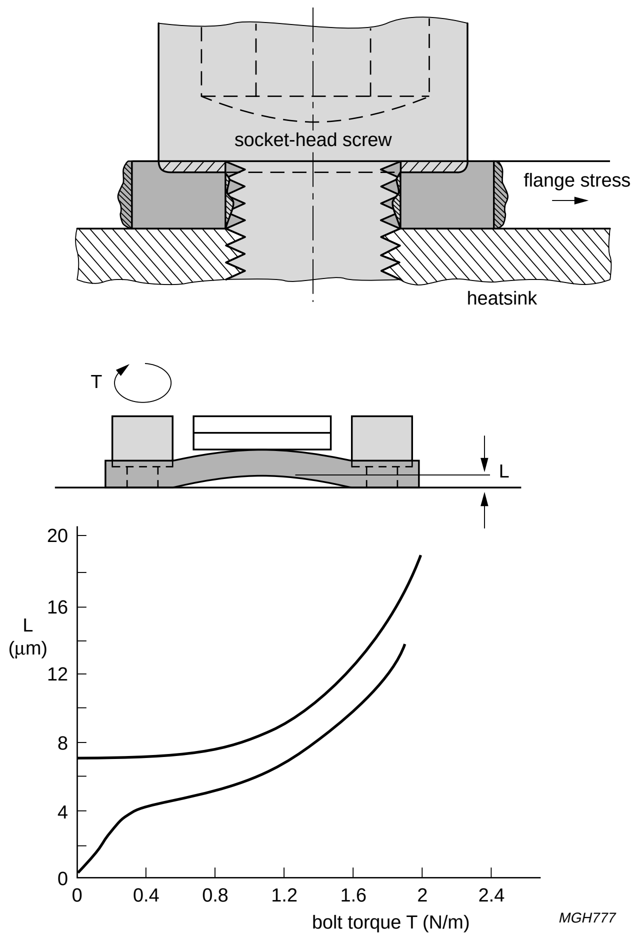

Fig.13 Above, plastic deformation in the flange. Below, how the centre of the flange tends to lift under excessive pressure.

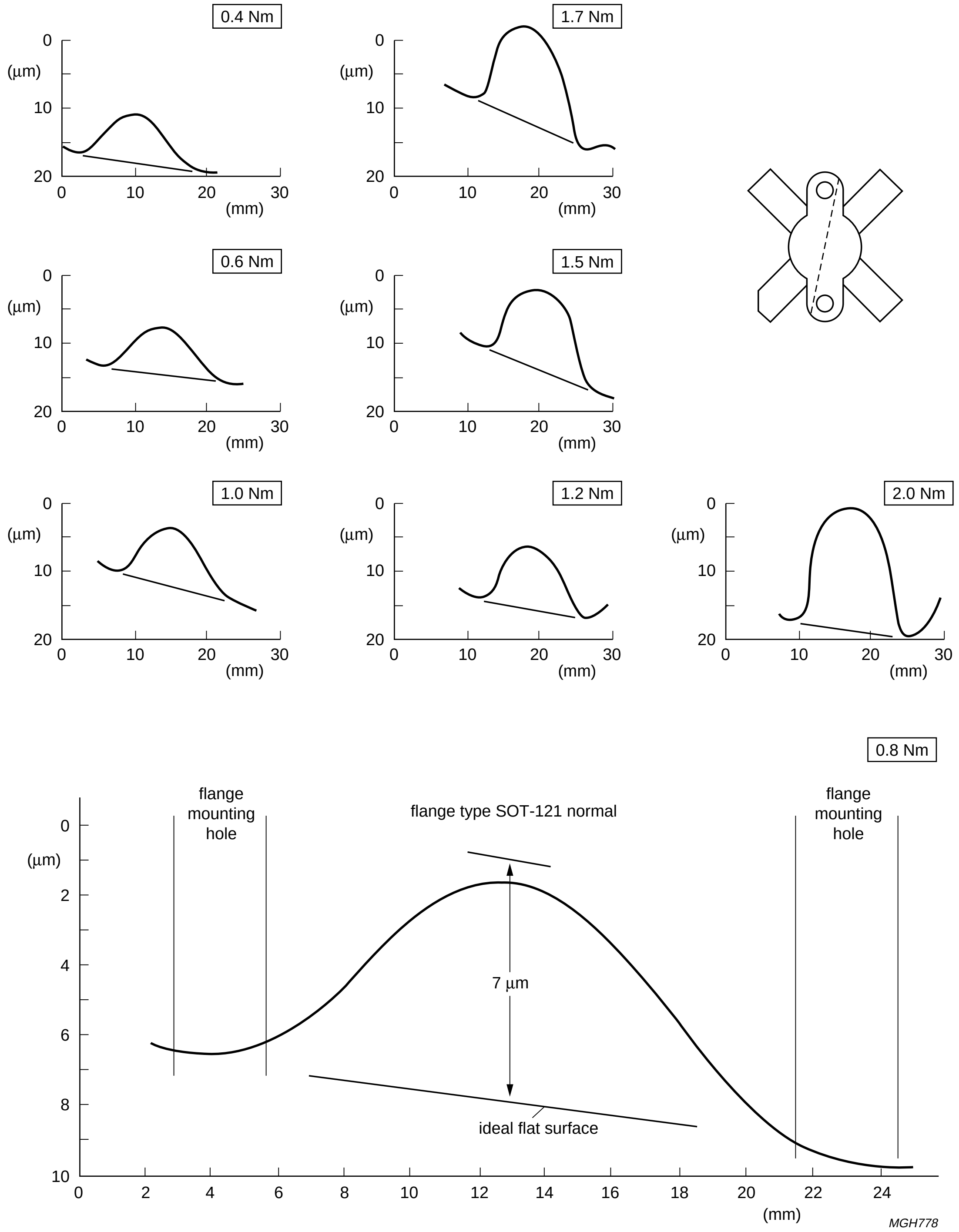

Fig.14 Measured deformation in an unlapped flange when steel M3 bolts are torqued in steps to 2,0 Nm. The curves have been smoothed to remove the effects of micro-asperities. The enlarged curve is for a torque of 0,8 Nm and shows a deformation of 7 µm at the centre.

11 CREEP

The deformation just described occurs immediately the stress is applied; under continued stress there is a further slow deformation that tends to reduce the applied stress. This slow deformation is known as creep.

Creep causes plastic strain to increase with time and, because the strain in a mounted transistor flange is constant, elastic strain decreases. Stress decreases as the elastic strain decreases. Figure 15 shows how stress reduces over time. It is, however, no more than an indication because relaxation speed is highly dependent on temperature, cyclic strain, work hardening and recrystallization. Under normal operating conditions temperature cycling will cause work hardening which will promote resistance to stress relaxation. On the other hand the cyclic strain imposed by temperature variations and the (more or less) elevated temperature of the flange during operation will tend to increase stress relaxation.

Our experience in temperature cycling (thermal fatigue) tests shows that relaxation reaches 30% in the first 100 hr and 50% in the first thousand. These tests are, of course, severer than normal operating conditions.

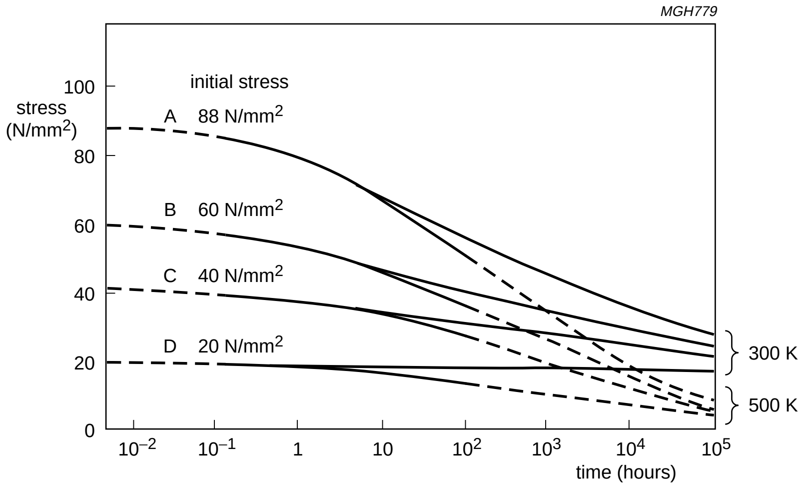

Fig.15 Typical creep curves in oxygen-free high conductivity copper. These are representative for the transistor flange copper but can only be considered as indicative because creep is also influenced by cyclic strains (temperature) such as occur in an operating transistor.

12 APPENDIX

12.1 Cavity test

The transistors were mounted on a water-cooled copper rod (30 mm dia.), the centre of the upper surface of which was maintained at 70°C. The upper surface was lapped to a flatness of <3 µm and a roughness r_a < 0,4 µm. The flange of one transistor was lapped to a flatness of <1 µm and a roughness r_a < 0,2 µm. The other transistor was not lapped and its flatness was 6 µm and its roughness r_a < 0,8 µm.

Dow Corning DC340 heatsink compound was used, except in one case where is was omitted to prove its efficacy. The transistors were adjusted to dissipate 150 W.

A circular cavity 1 mm deep was miled in the centre of the base of the flange. Initially it was 4 mm diameter and was increased in steps of 1 mm, burrs being removed at every stage. The percentage non-contacting surface area as a function of cavity diameter is shown in Fig.16. The amount of metal removed (1 mm depth) was insufficient to affect the bulk thermal properties of the flange.

Crystal temperatures were measured with a specially calibrated infra-red microscope. Heatsink and flange temperatures were measured with thermocouples places as in Fig.17. Thermocouple 1 was used as monitor and maintained at 70 °C.

Crystal temperatures were plotted, a typical scan being shown in Fig.18 (left), and average peak temperatures entered on thermal maps as in Fig.18 (right). Finally, curves were plotted of peak average temperatures at given points on the crystal against cavity size. The highest and lowest curves are those shown in Fig.19. Intervening curves have been omitted for clarity.

It will be seen that at a cavity of 7 mm, junction temperature has risen by less than 10 K and that it is not until the cavity is 9 mm or more that maximum junction temperature is exceeded. Clearly, lapping the transistor flange does reduce $R_{th\ mb\text{-}hs}$, but using heatsink compound has an even greater effect.

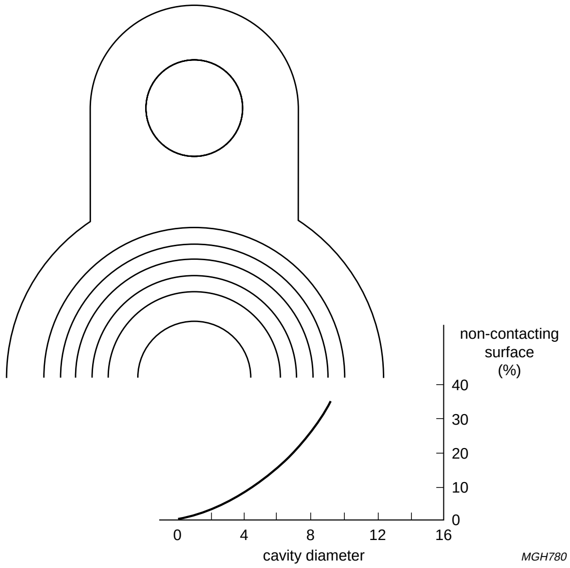

Fig.16 Contact surface area as a function of cavity size.

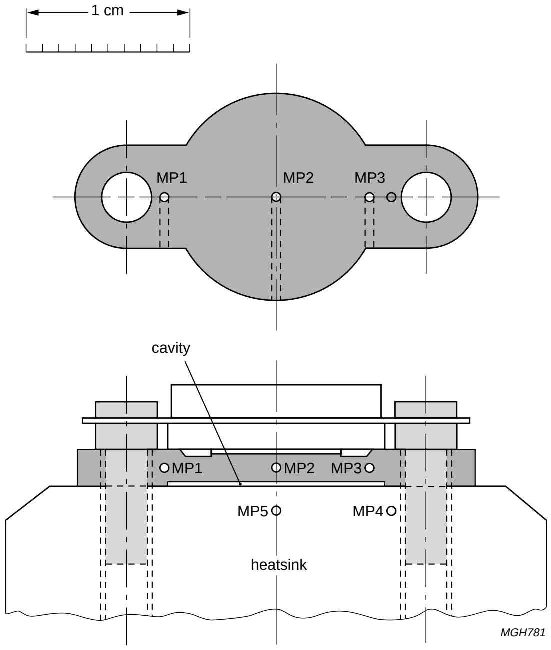

Fig.17 Placement of thermocouples for monitoring heatsink temperature.

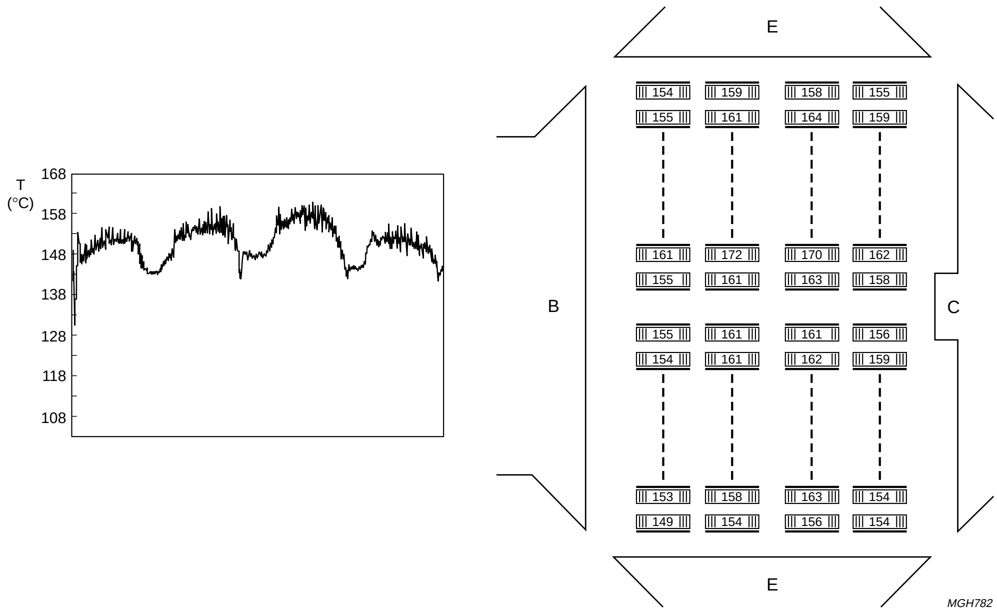

Fig.18 Junction temperature measurements. Left, a typical scan with the infrared microscope and right, a partial thermal map of average peak temperatures.

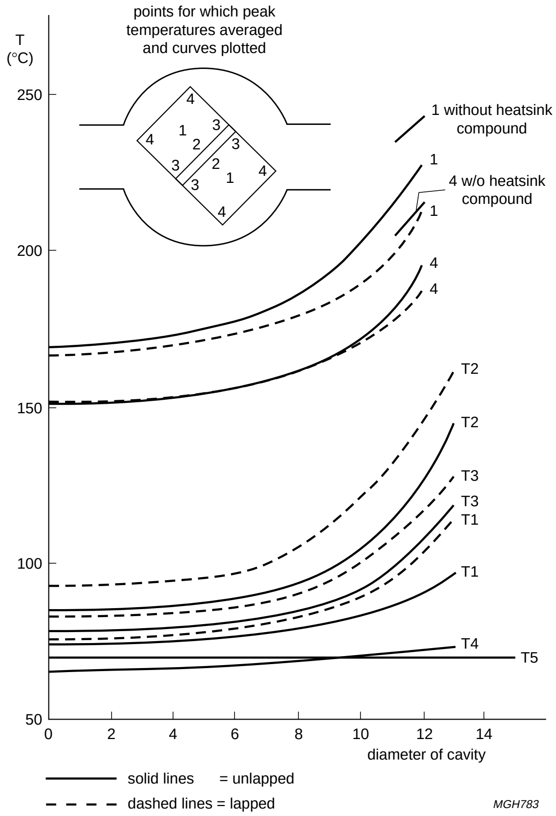

Fig.19 Curves of junction temperature against cavity size for a lapped transistor (solid line) and an unlapped transistor (broken line). It is not until the cavity is about 7 mm in diameter that junction temperature rises more than about 10 K.

Philips Semiconductors – a worldwide company

Argentina: see South America

Australia: 34 Waterloo Road, NORTH RYDE, NSW 2113,
Tel. +61 2 9805 4455, Fax. +61 2 9805 4466

Austria: Computerstr. 6, A-1101 WIEN, P.O. Box 213, Tel. +43 160 1010,
Fax. +43 160 101 1210

Belarus: Hotel Minsk Business Center, Bld. 3, r. 1211, Volodarski Str. 6,
220050 MINSK, Tel. +375 172 200 733, Fax. +375 172 200 773

Belgium: see The Netherlands

Brazil: see South America

Bulgaria: Philips Bulgaria Ltd., Energoproject, 15th floor,
51 James Bourchier Blvd., 1407 SOFIA,
Tel. +359 2 689 211, Fax. +359 2 689 102

Canada: PHILIPS SEMICONDUCTORS/COMPONENTS,
Tel. +1 800 234 7381

China/Hong Kong: 501 Hong Kong Industrial Technology Centre,
72 Tat Chee Avenue, Kowloon Tong, HONG KONG,
Tel. +852 2319 7888, Fax. +852 2319 7700

Colombia: see South America

Czech Republic: see Austria

Denmark: Prags Boulevard 80, PB 1919, DK-2300 COPENHAGEN S,
Tel. +45 32 88 2636, Fax. +45 31 57 0044

Finland: Sinikalliontie 3, FIN-02630 ESPOO,
Tel. +358 9 615800, Fax. +358 9 61580920

France: 51 Rue Carnot, BP317, 92156 SURESNES Cedex,
Tel. +33 1 40 99 6161, Fax. +33 1 40 99 6427

Germany: Hammerbrookstraße 69, D-20097 HAMBURG,
Tel. +49 40 23 53 60, Fax. +49 40 23 536 300

Greece: No. 15, 25th March Street, GR 17778 TAVROS/ATHENS,
Tel. +30 1 4894 339/239, Fax. +30 1 4814 240

Hungary: see Austria

India: Philips INDIA Ltd, Band Box Building, 2nd floor,
254-D, Dr. Annie Besant Road, Worli, MUMBAI 400 025,
Tel. +91 22 493 8541, Fax. +91 22 493 0966

Indonesia: see Singapore

Ireland: Newstead, Clonskeagh, DUBLIN 14,
Tel. +353 1 7640 000, Fax. +353 1 7640 200

Israel: RAPAC Electronics, 7 Kehilat Saloniki St, PO Box 18053,
TEL AVIV 61180, Tel. +972 3 645 0444, Fax. +972 3 649 1007

Italy: PHILIPS SEMICONDUCTORS, Piazza IV Novembre 3,
20124 MILANO, Tel. +39 2 6752 2531, Fax. +39 2 6752 2557

Japan: Philips Bldg 13-37, Kohnan 2-chome, Minato-ku, TOKYO 108,
Tel. +81 3 3740 5130, Fax. +81 3 3740 5077

Korea: Philips House, 260-199 Itaewon-dong, Yongsan-ku, SEOUL,
Tel. +82 2 709 1412, Fax. +82 2 709 1415

Malaysia: No. 76 Jalan Universiti, 46200 PETALING JAYA, SELANGOR,
Tel. +60 3 750 5214, Fax. +60 3 757 4880

Mexico: 5900 Gateway East, Suite 200, EL PASO, TEXAS 79905,
Tel. +9-5 800 234 7381

Middle East: see Italy

Netherlands: Postbus 90050, 5600 PB EINDHOVEN, Bldg. VB,
Tel. +31 40 27 82785, Fax. +31 40 27 88399

New Zealand: 2 Wagener Place, C.P.O. Box 1041, AUCKLAND,
Tel. +64 9 849 4160, Fax. +64 9 849 7811

Norway: Box 1, Manglerud 0612, OSLO,
Tel. +47 22 74 8000, Fax. +47 22 74 8341

Philippines: Philips Semiconductors Philippines Inc.,
106 Valero St. Salcedo Village, P.O. Box 2108 MCC, MAKATI,
Metro MANILA, Tel. +63 2 816 6380, Fax. +63 2 817 3474

Poland: Ul. Lukiska 10, PL 04-123 WARSZAWA,
Tel. +48 22 612 2831, Fax. +48 22 612 2327

Portugal: see Spain

Romania: see Italy

Russia: Philips Russia, Ul. Usatcheva 35A, 119048 MOSCOW,
Tel. +7 095 755 6918, Fax. +7 095 755 6919

Singapore: Lorong 1, Toa Payoh, SINGAPORE 1231,
Tel. +65 350 2538, Fax. +65 251 6500

Slovakia: see Austria

Slovenia: see Italy

South Africa: S.A. PHILIPS Pty Ltd., 195-215 Main Road Martindale,
2092 JOHANNESBURG, P.O. Box 7430 Johannesburg 2000,
Tel. +27 11 470 5911, Fax. +27 11 470 5494

South America: Al. Vicente Pinzon, 173, 6th floor,
04547-130 SÃO PAULO, SP, Brazil,
Tel. +55 11 821 2333, Fax. +55 11 821 2382

Spain: Balmes 22, 08007 BARCELONA,
Tel. +34 3 301 6312, Fax. +34 3 301 4107

Sweden: Kottbygatan 7, Akalla, S-16485 STOCKHOLM,
Tel. +46 8 632 2000, Fax. +46 8 632 2745

Switzerland: Allmendstrasse 140, CH-8027 ZÜRICH,
Tel. +41 1 488 2686, Fax. +41 1 488 3263

Taiwan: Philips Semiconductors, 6F, No. 96, Chien Kuo N. Rd., Sec. 1,
TAIPEI, Taiwan Tel. +886 2 2134 2865, Fax. +886 2 2134 2874

Thailand: PHILIPS ELECTRONICS (THAILAND) Ltd.,
209/2 Sanpavuth-Bangna Road Prakanong, BANGKOK 10260,
Tel. +66 2 745 4090, Fax. +66 2 398 0793

Turkey: Talatpasa Cad. No. 5, 80640 GÜLTEPE/ISTANBUL,
Tel. +90 212 279 2770, Fax. +90 212 282 6707

Ukraine: PHILIPS UKRAINE, 4 Patrice Lumumba str., Building B, Floor 7,
252042 KIEV, Tel. +380 44 264 2776, Fax. +380 44 268 0461

United Kingdom: Philips Semiconductors Ltd., 276 Bath Road, Hayes,
MIDDLESEX UB3 5BX, Tel. +44 181 730 5000, Fax. +44 181 754 8421

United States: 811 East Arques Avenue, SUNNYVALE, CA 94088-3409,
Tel. +1 800 234 7381

Uruguay: see South America

Vietnam: see Singapore

Yugoslavia: PHILIPS, Trg N. Pasica 5/v, 11000 BEOGRAD,
Tel. +381 11 625 344, Fax.+381 11 635 777

For all other countries apply to: Philips Semiconductors,
International Marketing & Sales Communications, Building BE-p, P.O. Box 218,
5600 MD EINDHOVEN, The Netherlands, Fax. +31 40 27 24825

Internet: http://www.semiconductors.philips.com

SCA57

Printed in The Netherlands

Date of release: 1998 Mar 23

Let's make things better.

Philips Semiconductors

PHILIPS